Trajectory Tracking Control of an Underactuated Autonomous Surface Craft in the Presence of Environmental Disturbances

[1]Wei Xie
Faculty of Science and Technology
University of Macau
Macau, China
weixie@um.edu.mo

[2]David Cabecinhas
Instituto Superior Técnico
Universidade de Lisboa
Lisboa, Portugal
dcabecinhas@isr.ist.utl.pt

[3]Rita Cunha
Instituto Superior Técnico
Universidade de Lisboa
Lisboa, Portugal
rita@isr.ist.utl.pt

[4]Carlos Silvestre
Faculty of Science and Technology
University of Macau
Macau, China
csilvestre@um.edu.mo

***Abstract*—This paper presents a nonlinear trajectory tracking controller for an autonomous surface craft under the presence of external time-varying environmental disturbances generated by wind, wave and ocean current. The proposed controller is able to drive the craft towards an arbitrarily small neighborhood of a smooth desired trajectory, obtaining global practical stability as the vehicle eventually remains within that neighborhood for all time. To demonstrate the efficacy of the designed control strategy, we give and analyze simulation results.**

***Index Terms*—underactuated surface craft, trajectory tracking, robust control, environmental disturbances.**

I. Introduction

In the past few years, autonomous surface crafts (ASCs) have been applied in many different areas, such as surveillance, search, marine data acquisition, among others [1], [2]. Unlike fully actuated vehicles, underactuated vehicles have less control inputs than degrees of freedom, raising new and challenging control problems. This paper presents a solution the problem of trajectory tracking for underactuated autonomous surface crafts which are actuated in force and torque, as the craft depicted in Fig. 1.

Diverse control strategies for stabilizing ASCs have been reported in the literature, such as in [3], where a tracking controller for an underactuated ship is proposed through the use of partial feedback linearization technique. The proposed controller drives the position of the ship exponentially to the desired trajectory without controlling the ship's course angle. By applying a combined integrator backstepping and averaging methodology, two tracking feedback control laws for an underactuated ship are developed in [4], which can exponentially drive the ship to an arbitrarily small neighborhood of the desired trajectory. The authors of [5] proposed a continuous position tracking controller for a surface vehicle that globally stabilizes the position and orientation errors to a ball centered at the origin with arbitrarily small radius. However, external disturbances are not considered in [4] and [5]. To reject external disturbances and achieve robust performance, in [6], [7], [8], under the assumption that disturbances are constants, disturbance observers are designed to compensate constant disturbances. To deal with external time-varying disturbances, a nonlinear disturbance estimator for a general nonlinear system was given in [9], with arbitrarily small estimation error. In [10], the authors employ a self-constructing fuzzy neural network to estimate unknown disturbances. Relevant work on robust control of surface crafts can also be found in [11] and [12].

Figure 1: Underactuated surface craft.

Motivated by our recent work [13] [14], this paper proposes a nonlinear robust tracking controller for an underactuated autonomous surface craft that achieves global practical stability. The stability of the overall closed-loop system is evaluated, and simulation results are presented to validate the efficacy of the developed control strategy.

The remainder of the paper is organized as follows. Section II introduces the notation used throughout the paper. The craft's kinematic and dynamic models and trajectory tracking problem are presented in Section III. The tracking controller and stability proof are given in Section IV. Section V presents and analyzes the simulation results. The contents of this paper are summarized in Section VI.

This work was supported by the Macao Science and Technology Development Fund under Grant FDCT/026/2017/A1, by the University of Macau, Macao, China, under Project MYRG2018-00198-FST, by the Fundação para a Ciência e a Tecnologia (FCT) through ISR under Grant LARSyS UID/EEA/50009/2019, FCT project LOTUS PTDC/EEI-AUT/5048/2014, and FCT Scientific Employment Stimulus grant CEECIND/04199/2017.

978-1-7281-1826-0/19/$31.00 ©2019 IEEE

II. Notation

In this paper, $\mathbb{R}^n$ represents the n-dimensional Euclidean space. A function g is of class C^n if the derivatives g', g'', $\ldots$, $g^{(n)}$ exist and are continuous. The norm of a vector $\mathbf{g} \in \mathbb{R}^n$ is defined as $\|\mathbf{g}\| = \sqrt{\mathbf{g}^\mathsf{T}\mathbf{g}}$. For a scalar $x \in \mathbb{R}$, its absolute value is denoted by $|x|$. The unit vectors $\mathbf{e}_1$ and $\mathbf{e}_2$ are introduced as $\mathbf{e}_1 = [1\ 0]^\mathsf{T}, \mathbf{e}_2 = [0\ 1]^\mathsf{T}$. In addition, Table I shows some main symbols and their corresponding descriptions used throughout the paper.

Table I: Symbols and descriptions

Symbol	Description
$\{I\}, \{B\}$	inertial frame and body frame
$\mathbf{d}_l, d_r$	damping coefficients
$\mathbf{b}_v, b_r$	disturbances
$\mathbf{p}$	craft's position expressed in $\{I\}$
$\mathbf{R}$	rotation matrix from $\{B\}$ to $\{I\}$
$\mathbf{v}$	linear velocity expressed in $\{B\}$
r	angular velocity expressed in $\{B\}$
I_z	craft's moment of inertia
m	craft's mass
T	thrust input
τ	torque input

III. Problem Formulation

This section presents the craft's model, and formulates the trajectory tracking problem.

A. Craft Modeling

The craft, shown in Fig. 1, is modeled as a rigid body subjected to external forces and torques. Consider a fixed inertia frame $\{I\}$ and a body-fixed frame $\{B\}$ attached to the craft's center of mass, as depicted in Fig. 2, we have the following kinematic equations [15], given as

$$\begin{aligned} \dot{\mathbf{p}} &= \mathbf{R}\mathbf{v} \\ \dot{\mathbf{R}} &= \mathbf{R}\mathbf{S}r \end{aligned} \tag{1}$$

where $\mathbf{p} = [x, y]^\mathsf{T}$ are the coordinates of the craft's center of mass, $\mathbf{v} = [u, v]^\mathsf{T}$ represents the linear velocity while r is angular velocity of the craft. The matrix $\mathbf{R}$ is the rotation matrix from $\{B\}$ to $\{I\}$, with

$$\mathbf{R} = \begin{bmatrix} \cos(\psi) & -\sin(\psi) \\ \sin(\psi) & \cos(\psi) \end{bmatrix}, \quad \mathbf{S} = \begin{bmatrix} 0 & -1 \\ 1 & 0 \end{bmatrix}.$$

where ψ is the orientation of the craft. The dynamic equations

$$\begin{aligned} \mathbf{M}\dot{\mathbf{v}} &= -\mathbf{S}r\mathbf{M}\mathbf{v} - \mathbf{v}_l\mathbf{d}_l + \mathbf{u}_1 T + \mathbf{R}^\mathsf{T}\mathbf{b}_v(t) \\ J\dot{r} &= -d_r r + \tau + b_r(t) \end{aligned} \tag{2}$$

where $\mathbf{M} = \mathrm{diag}(m - X_{\dot{u}}, m - Y_{\dot{v}})$, $J = I_z - N_{\dot{r}}$; m and I_z denote the mass and the inertial moment of the craft, respectively; $X_{\dot{u}}, Y_{\dot{v}}, N_{\dot{r}}$ represent the added masses; $\mathbf{d}_l = [X_u, Y_v]$ and $d_r = N_r$ are linear damping coefficients, $\mathbf{v}_l = \mathrm{diag}(u_r, v_r)$; T and τ represent thrust force and torque, respectively; external disturbances are denoted by $\mathbf{b}_v = [b_u(t), b_v(t)]^\mathsf{T}$ and $b_r(t)$, satisfying $|b_u(t)| \le \overline{b}_u, |b_v(t)| \le \overline{b}_v, |b_r(t)| \le \overline{b}_r$, where $\overline{b}_u, \overline{b}_v, \overline{b}_r$ are positive numbers.

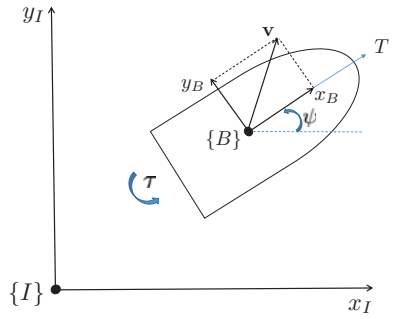

Figure 2: Illustration of $\{I\}$, $\{B\}$.

B. Trajectory Tracking Problem

The objective of trajectory tracking is to design a control law, including thrust force and torque, for an underactuated surface craft so that the craft can track a desired trajectory $\mathbf{p}_d(t) \in \mathbb{R}^2$ (a curve of class at least C^4), with arbitrarily small position error $\|\mathbf{p} - \mathbf{p}_d(t)\|$.

IV. Controller Design

In this section, a nonlinear trajectory tracking controller is proposed for an underactuated autonomous surface craft, which is robust to external environmental disturbances. We start the controller by defining the position error as

$$\mathbf{z}_1 = \mathbf{R}^\mathsf{T}(\mathbf{p} - \mathbf{p}_d)$$

which is expressed in the body frame. Then, we define our first Lyapunov candidate function as

$$V_1 = \frac{1}{2}\mathbf{z}_1^\mathsf{T}\mathbf{z}_1$$

and compute its time derivative, we have

$$\dot{V}_1 = -W_1(\mathbf{z}_1) + \mathbf{z}_1^\mathsf{T}\Big(\mathbf{v} - \mathbf{R}^\mathsf{T}\dot{\mathbf{p}}_d + k_1\mathbf{M}^{-1}\mathbf{z}_1\Big) \tag{3}$$

where $W_1(\mathbf{z}_1) = k_1\mathbf{z}_1^\mathsf{T}\mathbf{M}^{-1}\mathbf{z}_1$, k_1 is a positive number.

Taking a cue from [13], [16], a second error is defined as

$$\mathbf{z}_2 = \mathbf{v} - \mathbf{R}^\mathsf{T}\dot{\mathbf{p}}_d + k_1\mathbf{M}^{-1}\mathbf{z}_1 - \boldsymbol{\delta}$$

where $\boldsymbol{\delta} = [\delta_1, \delta_2]^\mathsf{T}$ is a constant vector whose properties will be specified later. Then, we rewrite (3) as

$$\dot{V}_1 = -W_1(\mathbf{z}_1) + \mathbf{z}_1^\mathsf{T}(\mathbf{z}_2 + \boldsymbol{\delta}).$$

Continuing with the backstepping procedure, a new Lyapunov candidate function is defined as

$$V_2 = V_1 + \frac{1}{2}\mathbf{z}_2^\mathsf{T}\mathbf{M}^2\mathbf{z}_2$$

with time derivative

$$\begin{aligned} \dot{V}_2 = &-W_2(\mathbf{z}_1, \mathbf{z}_2) + \mathbf{z}_1^\mathsf{T}\boldsymbol{\delta} + \mathbf{z}_2^\mathsf{T}\mathbf{M}\Big(- \mathbf{S}\mathbf{M}(\mathbf{R}^\mathsf{T}\dot{\mathbf{p}}_d + \boldsymbol{\delta})r \\ &+ \mathbf{M}\mathbf{S}\mathbf{R}^\mathsf{T}\dot{\mathbf{p}}_d r + \mathbf{e}_1 T - \mathbf{v}_l\mathbf{d}_l - \mathbf{M}\mathbf{R}^\mathsf{T}\ddot{\mathbf{p}}_d + k_1(\mathbf{v} - \mathbf{R}^\mathsf{T}\dot{\mathbf{p}}_d) \\ &+ k_2\mathbf{M}^{-1}\mathbf{z}_2\Big) + \mathbf{z}_2^\mathsf{T}\mathbf{M}\mathbf{R}^\mathsf{T}\mathbf{b}_v. \end{aligned} \tag{4}$$

where $W_2(\mathbf{z}_1, \mathbf{z}_2) = k_1\mathbf{z}_1^\top\mathbf{z}_1 + k_2\mathbf{z}_2^\top\mathbf{z}_2$, k_2 is a positive number.

Following [17], the inequality

$$|\chi| \le \chi \tanh(\chi/\epsilon) + \kappa\epsilon \tag{5}$$

is used, where $\kappa = 0.2785$, ϵ is any positive number. Then, we have

$$\mathbf{z}_2^\top\mathbf{M}\mathbf{R}^\top\mathbf{b}_v \le \mathbf{z}_2^\top\mathbf{M}\mathbf{R}^\top\boldsymbol{\beta}_1 + \kappa\epsilon$$

with

$$\boldsymbol{\beta}_1 = \Big[\overline{b}_u \tanh\Big(\mathbf{e}_1^\top\mathbf{R}\mathbf{M}^\top\mathbf{z}_2\overline{b}_u/\epsilon\Big), \overline{b}_v \tanh\Big(\mathbf{e}_2^\top\mathbf{R}\mathbf{M}^\top\mathbf{z}_2\overline{b}_v/\epsilon\Big)\Big]^\top.$$

Rewriting (4), we have

$$\dot{V}_2 \le -W_2(\mathbf{z}_1, \mathbf{z}_2) + \mathbf{z}_1^\top\boldsymbol{\delta} + \mathbf{z}_2^\top\mathbf{M}\Big(\boldsymbol{\alpha}r + \mathbf{e}_1 T + \boldsymbol{\eta}\Big) + \kappa\epsilon \tag{6}$$

with $\boldsymbol{\alpha} = -\mathbf{S}\mathbf{M}(\mathbf{R}^\top\dot{\mathbf{p}}_d + \boldsymbol{\delta}) + \mathbf{M}\mathbf{S}\mathbf{R}^\top\dot{\mathbf{p}}_d$,

$$\boldsymbol{\eta} = -\mathbf{v}_l\mathbf{d}_l - \mathbf{M}\mathbf{R}^\top\ddot{\mathbf{p}}_d + k_1(\mathbf{v} - \mathbf{R}^\top\dot{\mathbf{p}}_d) + k_2\mathbf{M}^{-1}\mathbf{z}_2 + \mathbf{R}^\top\boldsymbol{\beta}_1.$$

To cancel the first component of $(\boldsymbol{\alpha}r+\boldsymbol{\eta})$, we choose the thrust force as

$$T = -\mathbf{e}_1^\top(\boldsymbol{\alpha}r + \boldsymbol{\eta}). \tag{7}$$

Substituting (7) into (6), we have

$$\dot{V}_2 \le -W_2(\mathbf{z}_1, \mathbf{z}_2) + \mathbf{z}_1^\top\boldsymbol{\delta} + \mathbf{z}_2^\top\mathbf{M}\mathbf{e}_2\Big(\mathbf{e}_2(\boldsymbol{\alpha}r + \boldsymbol{\eta})\Big) + \kappa\epsilon.$$

Define the last error, angular velocity error, as

$$z_3 = \mathbf{e}_2(\boldsymbol{\alpha}r + \boldsymbol{\eta})$$

and define a new Lyapunov candidate function

$$V_3 = V_2 + \frac{1}{2}z_3^2.$$

Taking the time derivative of V_3, we obtain

$$\begin{aligned}\dot{V}_3 \le -W_3(\mathbf{z}_1, \mathbf{z}_2, z_3) + \mathbf{z}_1^\top\boldsymbol{\delta} + z_3\Big(&\mathbf{e}_2^\top\dot{\boldsymbol{\alpha}}r + \mathbf{e}_2^\top\boldsymbol{\alpha}\Big(-J^{-1}d_r r \\ &+ J^{-1}\tau + J^{-1}b_r(t)\Big) + \mathbf{e}_2^\top\dot{\boldsymbol{\eta}} + \mathbf{z}_2^\top\mathbf{M}\mathbf{e}_2 + k_3 z_3\Big) + \kappa\epsilon\end{aligned} \tag{8}$$

Notice that in $\dot{\boldsymbol{\eta}}$ there still exist unknown disturbances $\mathbf{b}_v$, and to emphasize the linear dependence on $\mathbf{b}_v$, we express $\dot{\boldsymbol{\eta}}$ as

$$\dot{\boldsymbol{\eta}} = \overline{\dot{\boldsymbol{\eta}}} + \frac{\partial\boldsymbol{\eta}}{\partial\mathbf{v}}\mathbf{R}^\top\mathbf{b}_v.$$

Furthermore, (8) can rewritten as

$$\begin{aligned}\dot{V}_3 \le -W_3(\mathbf{z}_1, \mathbf{z}_2, z_3) + \mathbf{z}_1^\top\boldsymbol{\delta} + z_3\Big(&\mathbf{e}_2^\top\dot{\boldsymbol{\alpha}}r + \mathbf{e}_2^\top\boldsymbol{\alpha}\Big(-J^{-1}d_r r \\ &+ J^{-1}\tau\Big) + \mathbf{e}_2^\top\overline{\dot{\boldsymbol{\eta}}} + \mathbf{z}_2^\top\mathbf{M}\mathbf{e}_2 + k_3 z_3\Big) + z_3\mathbf{e}_2^\top\boldsymbol{\alpha}J^{-1}b_r \\ &+ z_3\mathbf{e}_2^\top\frac{\partial\boldsymbol{\eta}}{\partial\mathbf{v}}\mathbf{R}^\top\mathbf{b}_v + \kappa\epsilon.\end{aligned} \tag{9}$$

Using inequality (5), we get

$$z_3\mathbf{e}_2^\top\frac{\partial\boldsymbol{\eta}}{\partial\mathbf{v}}\mathbf{R}^\top\mathbf{b}_v \le z_3\mathbf{e}_2^\top\frac{\partial\boldsymbol{\eta}}{\partial\mathbf{v}}\mathbf{R}^\top\boldsymbol{\beta}_2 + \kappa\epsilon$$

and

$$z_3\mathbf{e}_2^\top\boldsymbol{\alpha}J^{-1}b_r \le z_3\mathbf{e}_2^\top\boldsymbol{\alpha}J^{-1}\boldsymbol{\beta}_3 + \kappa\epsilon$$

with

$$\boldsymbol{\beta}_2 = \Big[\overline{b}_u \tanh\Big(\mathbf{e}_1^\top\mathbf{R}(\frac{\partial\boldsymbol{\eta}}{\partial\mathbf{v}})^\top\mathbf{e}_2 z_3/\epsilon\Big), \overline{b}_v \tanh\Big(\mathbf{e}_2^\top\mathbf{R}(\frac{\partial\boldsymbol{\eta}}{\partial\mathbf{v}})^\top\mathbf{e}_2 z_3/\epsilon\Big)\Big]$$

and

$$\beta_3 = \overline{b}_r \tanh\Big(\mathbf{e}_2^\top\boldsymbol{\alpha}J^{-1}\overline{b}_r z_3/\epsilon\Big).$$

Then, we can rewrite (9) as

$$\begin{aligned}\dot{V}_3 \le -W_3(\mathbf{z}_1, \mathbf{z}_2, z_3) + \mathbf{z}_1^\top\boldsymbol{\delta} + z_3\Big(&\mathbf{e}_2^\top\dot{\boldsymbol{\alpha}}r + \mathbf{e}_2^\top\boldsymbol{\alpha}\Big(-J^{-1}d_r r \\ &+ J^{-1}\tau\Big) + \mathbf{e}_2^\top\overline{\dot{\boldsymbol{\eta}}} + \mathbf{z}_2^\top\mathbf{M}\mathbf{e}_2 + k_3 z_3 + \mathbf{e}_2^\top\frac{\partial\boldsymbol{\eta}}{\partial\mathbf{v}}\mathbf{R}^\top\boldsymbol{\beta}_2 \\ &+ \mathbf{e}_2^\top\boldsymbol{\alpha}J^{-1}\beta_3\Big) + \kappa\epsilon_n.\end{aligned} \tag{10}$$

where $\epsilon_n = 3\epsilon$.

Choosing the torque as

$$\begin{aligned}\tau = -J(\mathbf{e}_2^\top\boldsymbol{\alpha})^{-1}\Big(&\mathbf{e}_2^\top\dot{\boldsymbol{\alpha}}r - \mathbf{e}_2^\top\boldsymbol{\alpha}J^{-1}d_r r + \mathbf{e}_2^\top\overline{\dot{\boldsymbol{\eta}}} + \mathbf{z}_2^\top\mathbf{M}\mathbf{e}_2 \\ &+ k_3 z_3 + \mathbf{e}_2^\top\frac{\partial\boldsymbol{\eta}}{\partial\mathbf{v}}\mathbf{R}^\top\boldsymbol{\beta}_2 + \mathbf{e}_2^\top\boldsymbol{\alpha}J^{-1}\beta_3\Big)\end{aligned} \tag{11}$$

to zero out $(\mathbf{e}_2^\top\dot{\boldsymbol{\alpha}}r + \mathbf{e}_2^\top\boldsymbol{\alpha}\Big(-J^{-1}d_r r + J^{-1}\tau\Big) + \mathbf{e}_2^\top\overline{\dot{\boldsymbol{\eta}}} + \mathbf{z}_2^\top\mathbf{M}\mathbf{e}_2 + k_3 z_3 + \mathbf{e}_2^\top(\partial\boldsymbol{\eta}/\partial\mathbf{v})\mathbf{R}^\top\boldsymbol{\beta}_2 + \mathbf{e}_2^\top\boldsymbol{\alpha}J^{-1}\beta_3)$. To avoid singularity in the control law, we need to guarantee

$$\mathbf{e}_2^\top\boldsymbol{\alpha} \ne 0$$

which is equivalent to

$$\mathbf{e}_1^\top\boldsymbol{\delta} \ne \frac{X_{\dot{u}} - Y_{\dot{v}}}{m - X_{\dot{u}}}(\mathbf{e}_1^\top\mathbf{R}^\top\dot{\mathbf{p}}_d).$$

To achieve this objective, we choose $\boldsymbol{\delta}$, such that

$$|\delta_1| > \Big|\frac{X_{\dot{u}} - Y_{\dot{v}}}{m - X_{\dot{u}}}\Big| v_{\max}$$

where $v_{\max} \ge \|\dot{\mathbf{p}}_d\|$.

Substituting (11) into (10), we get

$$\dot{V}_3 \le -W_3(\mathbf{z}) + \mathbf{z}_1^\top\boldsymbol{\delta} + \kappa\epsilon_n. \tag{12}$$

where $\mathbf{z} = [\mathbf{z}_1^\top, \mathbf{z}_2^\top, z_3]^\top$, $W_3(\mathbf{z}) = k_1\mathbf{z}_1^\top\mathbf{z}_1 + k_2\mathbf{z}_2^\top\mathbf{z}_2 + k_3 z_3^2$, k_3 is a positive number. The main result of this work is summarized in the following theorem.

Theorem 1: Let the craft's model be described by (1)-(2) and $\mathbf{p}_d \in C^4$ be the reference trajectory whose time derivatives are bounded. Considering the control inputs, (7), (11), the constant vector $\boldsymbol{\delta} = [\delta_1, \delta_2]^\top$ is chosen such that

$$|\delta_1| > \Big|\frac{X_{\dot{u}} - Y_{\dot{v}}}{m - X_{\dot{u}}}\Big| v_{\max}.$$

For any initial condition, the tracking error $\|\mathbf{z}\|$ will be driven to a ball centered at the origin with radius $\sqrt{\kappa\epsilon_n/\lambda + \|\boldsymbol{\delta}\|^2/(2\varepsilon\lambda)}$, where $k_1 > \varepsilon/2 > 0$, $\lambda = \min\{k_1 - \varepsilon/2, k_2, k_3\}$, which can be made arbitrarily small by increasing control gains k_1, k_2, k_3 and reducing $\epsilon_n, \|\boldsymbol{\delta}\|$.

Proof 1: We apply Young inequality to (12), and conclude that

$$\begin{aligned}\dot{V}_3 &\le -\Big(k_1 - \frac{\varepsilon}{2}\Big)\mathbf{z}_1^\top\mathbf{z}_1 - k_2\mathbf{z}_2^\top\mathbf{z}_2 - k_3 z_3^2 + \Big(\kappa\epsilon_n + \frac{\|\boldsymbol{\delta}\|^2}{2\varepsilon}\Big) \\ &\le -\lambda\|\mathbf{z}\|^2 + \Big(\kappa\epsilon_n + \frac{\|\boldsymbol{\delta}\|^2}{2\varepsilon}\Big)\end{aligned}$$

where $k_1 > \varepsilon/2, \varepsilon > 0$ and $\lambda = \min\{k_1 - \varepsilon/2, k_2, k_3\}$. I which we can further get that $\dot{V}_3$ is strictly negative de for $\|\mathbf{z}\|^2 > \kappa\epsilon_n/\lambda + \|\boldsymbol{\delta}\|^2/(2\varepsilon\lambda)$, leading to the conclusion $\|\mathbf{z}\|$ is uniformly bounded by $\sqrt{\kappa\epsilon_n/\lambda + \|\boldsymbol{\delta}\|^2/(2\varepsilon\lambda)}$.

V. Simulation Results

To validate the efficacy of the developed controller he simulation results are given in this section. The main pa eters used for simulation are presented in Table II, the di bances are chosen as $\mathbf{b}_v(t) = [\bar{b}_u \cos(t), \bar{b}_v \sin(t)]^\mathsf{T}$ (N), b_r $\bar{b}_r \sin(t)$ (N · m), with $\bar{b}_u = 10, \bar{b}_v = 8, \bar{b}_r = 1$.

Table II: Parameters used in simulation

Parameter	Value	Parameter	Value
m	25	$Y_{\dot{v}}$	-15.25
I_z	5.0715	$N_{\dot{r}}$	-1.23
X_u	10.7797	k_1	60
Y_v	16.9827	k_2	10
N_r	9	k_3	15
$X_{\dot{u}}$	−5.91	$\boldsymbol{\delta}$	$[-0.31, 0]^\mathsf{T}$

The desired trajectory is an ellipse defined as

$$\mathbf{p}_d(t) = \begin{bmatrix} d_1 \cos(\omega t) \\ d_2 \sin(\omega t) \end{bmatrix} \text{(m)}$$

where $d_1 = 10, d_2 = 6, \omega = 0.1$ (rad/s). Fig. 3 contrasts the actual and desired trajectories, showing that the craft tracks the desired trajectory closely. Correspondingly, the time evolution of $\|\mathbf{z}_1\|$, denoted by the blue line, is depicted in Fig. 4. In steady state, its root mean square error (RMSE) and standard deviation (SD) are 0.163(m) and 0.029(m), respectively. In order to show the developed control methodology is capable of rejecting the external disturbances, Fig. 4 also displays the time evolution of $\|\mathbf{z}_1\|$ for an identically derived controller but without the disturbance rejection terms, represented by the red line. When it arrives at the steady state, its RMSE and SD are 0.335(m) and 0.095(m), respectively, which are much larger that these obtained using the proposed dealing with disturbances approach, therefore justifying the use of the proposed control structure. Moreover, Fig. 5 shows the time evolution of $\mathbf{e}_2^\mathsf{T}\boldsymbol{\alpha}$, from where we can see it is always larger than zero, guaranteeing τ, defined in (11), is well-defined.

VI. Conclusion

This paper proposes a solution to the trajectory tracking problem for an underactuated autonomous surface craft in the presence of external environmental disturbances. The developed nonlinear tracking controller can stabilize the craft to an arbitrarily small neighborhood of the desired trajectory, obtaining global practical stability. Simulation results are given and analyzed, validating the efficacy of the proposed control laws.

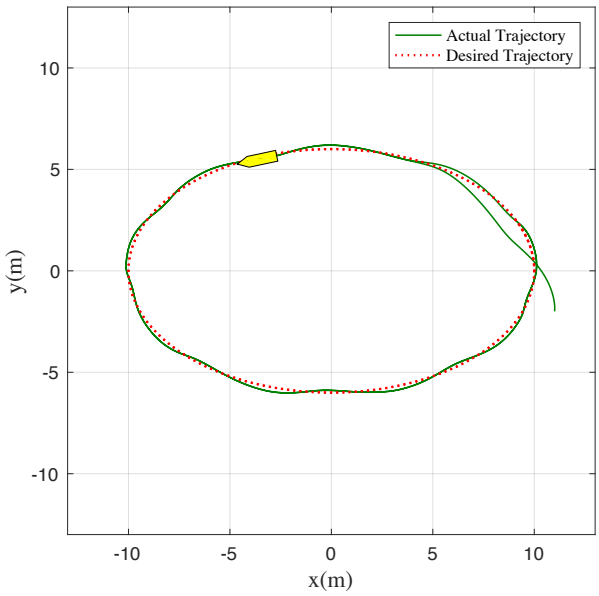

Figure 3: Time evolution of the actual craft position and the desired trajectory.

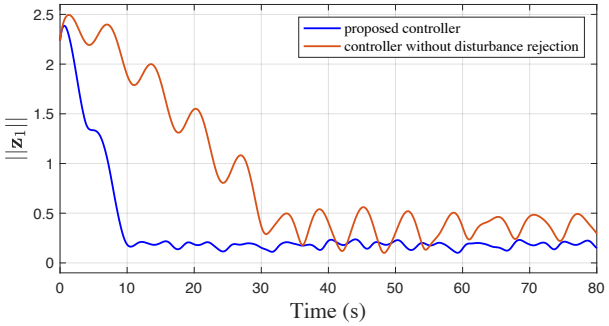

Figure 4: Time evolution of $\|\mathbf{z}_1\|$ with and without dealing with external disturbances.

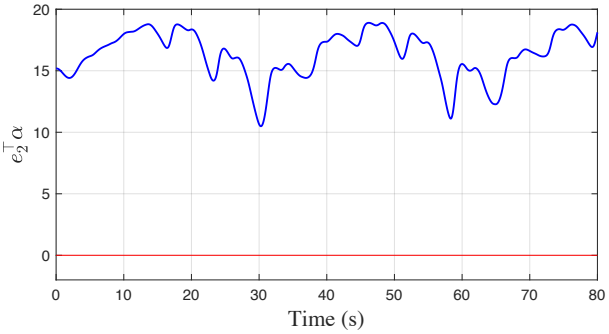

Figure 5: Time evolution of $\mathbf{e}_2^\mathsf{T}\boldsymbol{\alpha}$ which is always nonzero.

References

[1] S. Campbell, W. Naeem, and G. W. Irwin. A review on improving the autonomy of unmanned surface vehicles through intelligent collision avoidance manoeuvres. *Annual Reviews in Control*, 36(2): 267 - 283, 2012.

[2] J. Alves, P. Oliveira, R. Oliveira, A. Pascoal, M. Rufino, L. Sebastiao, and C. Silvestre. Vehicle and Mission Control of the DELFIM Autonomous Surface Craft. *14th Mediterranean Conference on Control and Automation*, 1-6, 2006.

[3] S. P. Berge, K. Ohtsu, and T. I. Fossen. Nonlinear tracking control of underactuated ships minimizing the cross-track error. *Proceedings of the IFAC Conference on Control Applications in Marine Systems*, 141-147, 1998.

[4] K. Y. Pettersen, and H. Nijmeijer. Global practical stabilization and tracking for an underactuated ship-a combined averaging and backstepping approach. *Modeling Identification and Control*, 20(4): 189-200, 1999.

[5] A. Behal, D. M. Dawson, B. Xian, and P. Setlur. Adaptive tracking control of underactuated surface vessels. *Proceedings of the 2001 IEEE International Conference on Control Applications*, 645-650, 2001.

[6] J. Almeida, C. Silvestre, and A. Pascoal. Cooperative control of multiple surface vessels in the presence of ocean currents and parametric model uncertainty. *International Journal of Robust and Nonlinear Control*, 20(14): 1549-1565, 2010.

[7] D. Lu, W. Xie, D. Cabecinhas, R. Cunha, and C. Silvestre. Path Following Controller Design for an Underactuated Hovercraft with External Disturbances. *19th International Conference on Control, Automation and Systems*, 2019.

[8] H. Aschemann, and A. Rauh. Nonlinear control and disturbance compensation for underactuated ships using extended linearisation techniques. *8th IFAC Conference on Control Applications in Marine Systems*, 177-172, 2010.

[9] K. D. Do. Practical control of underactuated ships. *Ocean Engineering*, 37(13): 1111-1119, 2010.

[10] N. Wang and M. Joo Er. Self-Constructing Adaptive Robust Fuzzy Neural Tracking Control of Surface Vehicles With Uncertainties and Unknown Disturbances. *IEEE Transactions on Control Systems Technology*, 23(3): 991-1002, 2015.

[11] D. Cabecinhas, P. Batista, P. Oliveira, and C. Silvestre. Hovercraft Control With Dynamic Parameters Identification. *IEEE Transactions on Control Systems Technology*, 26(3): 785-796, 2018.

[12] D. Belleter, M. A. Maghenem, C. Paliotta, and K. Y. Pettersen. Observer based path following for underactuated marine vessels in the presence of ocean currents: A global approach. *Automatica*, 100: 123-134, 2019.

[13] W. Xie, D. Cabecinhas, R. Cunha, and C. Silvestre. Robust Motion Control of an Underactuated Hovercraft. *IEEE Transactions on Control Systems Technology*, 27(5), 2195-2208, 2019.

[14] R. Zhao, W. Xie, P.K. Wong, D. Cabecinhas, and C. Silvestre. Robust Ride Height Control for Active Air Suspension Systems With Multiple Unmodeled Dynamics and Parametric Uncertainties. *IEEE Access*, 7: 59185-59199, 2019.

[15] T. I. Fossen. Marine Control Systems: Guidance, Navigation and of Ships, Rigs and Underwater Vehicles. *Marine Cybernetics, Trondheim, Norway*, 2002.

[16] A. P. Aguiar, and J. P. Hespanha. Trajectory-Tracking and Path-Following of Underactuated Autonomous Vehicles With Parametric Modeling Uncertainty. *IEEE Transactions on Automatic Control*, 52(8): 1362-1379, 2007.

[17] M. M. Polycarpou. Stable Adaptive Neural Control Scheme for Nonlinear Systems. *IEEE Transactions on Automatic Control*, 41(3): 447-451, 1996.